10 November 2000

ELSEVIER

Chemical Physics Letters 330 (2000) 423–432

CHEMICAL PHYSICS LETTERS

www.elsevier.nl/locate/cplett

Theoretical analysis of the vanadyl pyrophosphate $(VO)_2P_2O_7$ ^{31}P NMR spectra

L.M. Lawson Daku [a,b,*], S.A. Borshch [a,b,1], V. Robert [a,b], B. Bigot [a,b]

[a] *Institut de Recherches sur la Catalyse, UPR 5401, 2, avenue Albert Einstein, 69626 Villeurbanne Cedex, France*
[b] *Ecole normale supérieure de Lyon, Laboratoire de Chimie Théorique, 46, allée d'Italie, 69364 Lyon Cedex 07, France*

Received 11 April 2000; in final form 22 August 2000

Abstract

We present a theoretical analysis of the temperature dependence of the vanadyl pyrophosphate $VO_2P_2O_7$ ^{31}P NMR spectra. Four distinct phosphorus sites responsible for four signals are identified in the crystal structure. The magnetic states of the crystal are described by two alternative models: the spin ladder and the dimer chain. Within both models, finite clusters with and without periodic conditions are considered. The fit of the experimental NMR data allows us to define combinations of hyperfine coupling parameters which are found to be similar in both spin models. © 2000 Elsevier Science B.V. All rights reserved.

1. Introduction

The vanadyl pyrophosphate compound $(VO)_2P_2O_7$ (VPO) attracts much attention from the physical and chemical communities, but from rather different points of view. The chemical importance of VPO is dictated by the fact that it represents the most active phase of the vanadium–phosphorus–oxide catalysts for the selective oxidation of butane and butene to maleic anhydride [1]. Numerous experimental and theoretical studies were performed to elucidate the electronic and structural properties of this system and, finally, to identify the nature of the catalytic active site. In solid state physics, the interest to VPO has grown from its intriguing magnetic properties. It has long been considered as a first example of antiferromagnetic spin ladder [2–7]. This low-dimensional magnetic system (Fig. 1(1)) is characterized by two exchange parameters, corresponding to the nearest-neighbour interactions: along the infinite chain ($J_{\parallel}$) and along the rungs of a ladder geometry ($J_{\perp}$). However, the magnetic susceptibility of the VPO can be accurately fitted not only by the spin ladder model, but also by a rather different model, namely the dimer chain [2,7]. For the latter, the one-dimensional chain is described by two alternating exchange parameters J_1 and J_2 (Fig. 1(1)). It is clear that these two models correspond to quite different schemes of exchange interaction.

Although, the spin ladder model visually seems more natural for the VPO (Fig. 1(2)), latest quantum–chemical [8] and experimental (inelastic neutron scattering) [9,10] studies favour the dimer chain.

* Corresponding author. Fax: +33-4-72-44-53-99.
E-mail addresses: mlawson@ens-lyon.fr (L.M. Lawson Daku), borchtch@catalyse.univ-lyon1.fr (S.A. Borshch).
[1] Corresponding author.

0009-2614/00/$ - see front matter
PII: S0009-2614(00)01102-7

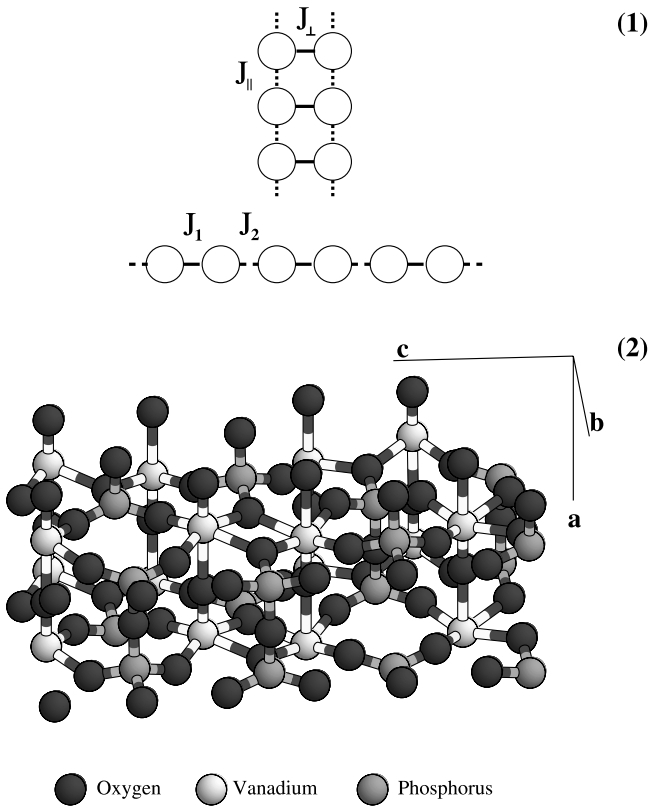

Fig. 1. (1) The two concurrent interactions schemes postulated for the VPO system. They correspond to the spin ladder model (top) and the dimer chain model (bottom). (2) The unit cell of VPO. It contains 104 atoms. This figure shows its idealized structure as proposed by Thompson et al. [11].

Among all the experimental methods used in the VPO studies, the ^{31}P NMR occupies a special place, since it gives access to the local characteristics of the electronic structure. NMR was widely used along different VPO research directions. The first ^{31}P NMR data for VPO were obtained by Li et al. with the spin echo technique [12]. A very broad band was observed around 2500 ppm. However, more recent studies of Tuel [13] and Yamauchi [14] showed the presence of four signals with different temperature dependences. It suggests the presence of four types of phosphorus atom in the solid with different hyperfine coupling with paramagnetic vanadium centers. It is well known that the interpretation of the NMR data for a magnetically coupled system such as VPO must be based on the analysis of the exchange interactions [15,16]. In order to describe the temperature dependence of the NMR paramagnetic shift, one needs to know the energy spectrum and the eigenfunctions of electronic spin levels.

Recently, we performed quantum–chemical calculations of molecular models of VPO in the diamagnetic state (all vanadium atoms are in d^0 electronic configuration) [17]. In the present Letter, we want to analyze the temperature dependence of VPO NMR spectroscopy data on the base of the real (with some simplifications) VPO structure. We will identify four different types of phosphorus atom and define dominating hyperfine interactions for them. The pathways of the exchange interactions between vanadium ions will be considered either within the spin ladder model or within the dimer chain model. For both cases, we firstly study a finite cluster and then impose periodic conditions.

2. Theoretical model

The hyperfine interaction in paramagnetic systems represents usually the main contribution to the observed NMR chemical shifts. In the case of a nucleus sensing only one paramagnetic center indexed by i, the expression for this contribution is [16]

$$\delta_{i,\mathrm{para}}(T) = \frac{g\mu_B}{g_\mathrm{I}\mu_N}\frac{A_i}{3k_BT} \frac{\sum_n K_i(n)S_n(S_n+1)(2S_n+1)\exp(-E_n/k_BT)}{\sum_n (2S_n+1)\exp(-E_n/k_BT)}, \quad (1)$$

where A_i is the hyperfine coupling constant, g the electronic g-factor, and g_I is the nuclear gyromagnetic factor. The summation runs over all energy levels E_n characterized by the total spin S_n. The projection coefficients $K_i(n)$ are given

$$K_i(n) = \frac{\langle S_n|\vec{s}_i\cdot\vec{S}|S_n\rangle}{\langle S_n|\vec{S}\cdot\vec{S}|S_n\rangle}, \quad (2)$$

where $\vec{s}_i$ is the spin operator of the center i and $\vec{S}$ is the total spin operator. In order to simplify the relation (1) and derived expressions, we introduce the quantity

$$F_i(T) = \frac{\sum_n K_i(n)S_n(S_n+1)(2S_n+1)\exp(-E_n/k_BT)}{\sum_n (2S_n+1)\exp(-E_n/k_BT)} \quad (3)$$

which gives the temperature dependence of the spin density on the paramagnetic center i. Eq. (1) now reads

$$\delta_{\mathrm{para}}(T) = \frac{\mathscr{C}A_iF_i(T)}{T}, \quad (4)$$

with $\mathscr{C} = g\mu_B/(3g_I\mu_Nk_B)$. If the nucleus sees more than one center, Eq. (4) is replaced by

$$\delta_{\mathrm{para}}(T) = \frac{\mathscr{C}}{T}\sum_i A_iF_i(T), \quad (5)$$

where now the summation runs over all paramagnetic centers. As it directly follows from (1)–(5), the calculation of the hyperfine shift needs the knowledge of energies E_n and eigenfunctions $|S_n\rangle$ of the spin levels.

The spin system of VPO is formed by interacting spins $s_i = 1/2$, corresponding to vanadium atoms in oxidation state +IV (electronic configuration d^1). We consider the two models of exchange interaction in VPO mentioned in Section 1. In the case of spin ladder hypothesis, the spin subsystem of VPO is described by the Heisenberg Hamiltonian

$$\mathscr{H}_1 = J_\perp\sum_{k=1}^{\infty}\vec{s}_{2k-1}\cdot\vec{s}_{2k} + J_\parallel\sum_{k=1}^{\infty}\left(\vec{s}_{2k-1}\cdot\vec{s}_{2k+1}+\vec{s}_{2k}\cdot\vec{s}_{2k+2}\right). \quad (6)$$

This model takes into account two types of exchange interaction. The $J_\perp$ parameter is responsible for the indirect exchange through di–μ–oxo bridges along $\vec{c}$-direction, and the $J_\parallel$ describes the exchange in $\mathrm{V=O\ldots V=0}$ units along the $\vec{a}$-direction (Fig. 1(2)).

The magnetic susceptibility data were successfully fitted on the base of this model with $J_\parallel = 90.7$ K and $J_\perp = 90.1$ K [7].

The dimer chain model supposes that the exchange through vanadyl oxygens is negligible, but that the interaction through O–P–O bridges in the $\vec{c}$-direction is important. Although this pathway corresponds to a longer V–V distance, recent experimental data [9] and quantum–chemical estimations agree with this statement [8]. The corresponding Heisenberg Hamiltonian is

$$\mathscr{H}_2 = J_1\sum_{k=1}^{\infty}\vec{s}_{2k-1}\cdot\vec{s}_{2k} + J_2\sum_{k=1}^{\infty}\vec{s}_{2k}\cdot\vec{s}_{2k+1}. \quad (7)$$

The satisfactory description of magnetic data was achieved with $J_1 = 128.9$ and $J_2 = 93.1$ K [7].

The Hamiltonians (6) and (7) can be diagonalized exactly in the case of a finite number of centers. In order to handle infinite systems, different approximation schemes can be used. For both spin models, we considered finite clusters with 2×6 spin centers. As was shown earlier by Barnes and Riera [7], clusters of such size give a good estimate of bulk susceptibility. In order to improve this description, we also considered clusters of the same size, but with periodic conditions. We will show below that both approximations give very close results.

Next, we must choose the most important hyperfine interactions defining the paramagnetic shift. It is done by inspecting the crystal structure of VPO. The real structure of VPO, whose determination was firstly addressed by Gorbunova and Linde [18] and recently precised by Nguyen et al. [19], shows a complex packing. For our purposes, we consider rather the simplified model proposed by Thompson et al. [11]. This idealized model preserves the equivalence of atoms found in the real structure and removes minor variations in bond lengths and bond angles. Next, let us recall that for a nucleus, the magnitude of the hyperfine interaction is defined by the transferred spin density which in its turn depends predominantly on the nucleus distance to the paramagnetic centers. Therefore, the most important factor to be taken into account in the estimation of the hyperfine interactions is the distances between a ^{31}P nucleus and magnetic vanadium centers. If we limit ourselves to distances less than 4 Å, it is easy to find two types of phosphorus atom (Fig. 2). For one of them the shortest distances to vanadium atoms are 3.15 (twice), 3.34 and 3.41 Å. For the second one, these distances are: 3.23 (twice), 3.34 and 3.41 Å.

We introduce four different hyperfine constants which depend only on the distances (Table 1).

However, all vanadium atoms are not equivalent. If we consider only the first coordination sphere, the difference appears in the relative orientation of the vanadyl group. Let us note the hyperfine constants for vanadium atoms with vanadyl bond up and down by superscripts + and −, respectively. Finally, we obtain four types of phosphorus atom characterized by the following combinations of the hyperfine constants

Table 1
The four different hyperfine coupling constants obtained using the ^{31}P–V distances as criteria

Coupling constant	A_1	A_2	A_3	A_4
Distance (Å)	3.15	3.23	3.34	3.41

$$\begin{array}{ll} \mathrm{I} \leftrightarrow 2A_1^+, A_3^+, A_4^- & \mathrm{II} \leftrightarrow 2A_1^-, A_3^-, A_4^+ \\ \mathrm{III} \leftrightarrow 2A_2^+, A_3^-, A_4^+ & \mathrm{IV} \leftrightarrow 2A_2^-, A_3^+, A_4^- \end{array}$$

and for which paramagnetic contributions read

$$\begin{aligned} \delta_{\mathrm{para}}^{\mathrm{I}}(T) &= \frac{\mathscr{C}}{T}\left[2A_1^+F_1^+(T) + A_3^+F_3^+(T) + A_4^-F_4^-(T)\right], \\ \delta_{\mathrm{para}}^{\mathrm{II}}(T) &= \frac{\mathscr{C}}{T}\left[2A_1^-F_1^-(T) + A_3^-F_3^-(T) + A_4^+F_4^+(T)\right], \\ \delta_{\mathrm{para}}^{\mathrm{III}}(T) &= \frac{\mathscr{C}}{T}\left[2A_2^+F_2^+(T) + A_3^-F_3^-(T) + A_4^+F_4^+(T)\right], \\ \delta_{\mathrm{para}}^{\mathrm{IV}}(T) &= \frac{\mathscr{C}}{T}\left[2A_2^-F_2^-(T) + A_3^+F_3^+(T) + A_4^-F_4^-(T)\right]. \end{aligned} \tag{8}$$

In our approach, we distinguish phosphorus atoms only by their distances to the magnetic vanadium centers and the nature of these latters. However, the transferred spin density at a phosphorus atom can also depend on its pathway. If one takes into account also the V–O–P angles, the number of non-equivalent phosphorus atoms in the elementary cell is equal to eight.

Now, our goal is to fit the observed temperature dependent NMR signals using Eq. (8) and to determine the hyperfine parameters $A_i^{\pm}$. The functions $F_i^{\pm}$ will be calculated within the different approximation schemes mentioned above.

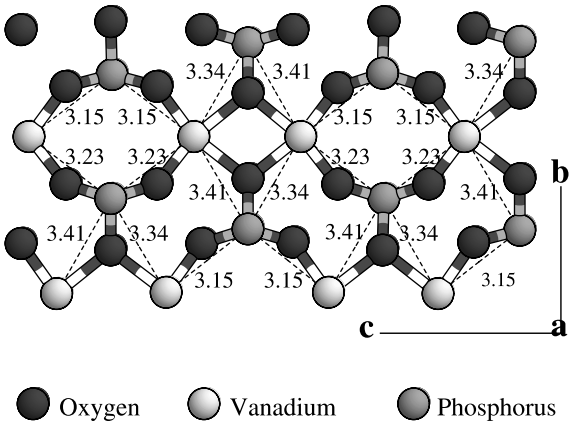

Fig. 2. A view from the top of the unit cell associated with the idealized structure, the shortest ^{31}P–V distances are indicated by [11].

3. Results and discussion

In order to fit the NMR data of the exchange coupled system VPO, we need to know the values

of the exchange constants. In principle, they can also be used as fit variables, but this increases the number of variables. In agreement with the results of the magnetic susceptibility studies, we took for the spin ladder model $J_{\parallel} = J_{\perp} = 90$ K [7]. For the dimer chain model, we took the parameters found from inelastic neutron scattering experiments $J_1 = 119$ and $J_2 = 101$ K [9].

In both models, we considered clusters containing six dimers, i.e., 12 magnetic centers, with or without periodic conditions. Using the values of the coupling constants mentioned above, the Hamiltonians (6) and (7) have been diagonalized within the individual subspaces of total electronic spin $S = 0, \ldots, 6$. The knowledge of the eigenfunctions allowed us to readily evaluate the projection coefficients K_i (see Appendix A). We thus can adjust the NMR data using the Eq. (8).

We took as estimates of the functions $F_i^{\pm}(T)$ in Eq. (8) those resulting from the diagonalization of the model Hamiltonians. Actually, for infinite model systems, those functions which are equivalent to a common one we note $F_{\infty}(T)$ (see Appendix A). In the case of finite clusters, this equivalence is not respected and we must choose the paramagnetic centers which donate spin density to the phosphorus atoms. The most convenient choice is to take for each model system a paramagnetic center located in the middle of the cluster, close to a bisecting plane (for the dimer chain model, this plane is parallel to the $(\vec{a}, \vec{b})$ plane, and for the spin ladder model, it is parallel to the $(\vec{b}, \vec{c})$ plane). The corresponding functions $F_i(T)$ are taken as estimates of $F_{\infty}(T)$. With this choice, the errors due to the clusters finite size are minimal. When dealing with systems with periodic conditions, the quantities $F_i(T)$ are identical (see Appendix A) and also taken as estimates of $F_{\infty}(T)$. Fig. 3 shows the plot of the functions $F_{\infty}(T)$ obtained for the spin ladder and dimer chain models, with and without periodic periodic conditions. For each model, both approximations give nearly identical results, slight differences occur only at low temperatures. The values taken by $F_{\infty}(T)$ for the spin ladder model are lower than those obtained for the dimer chain model. At high temperatures, this gap between the two families of curves remains almost constant.

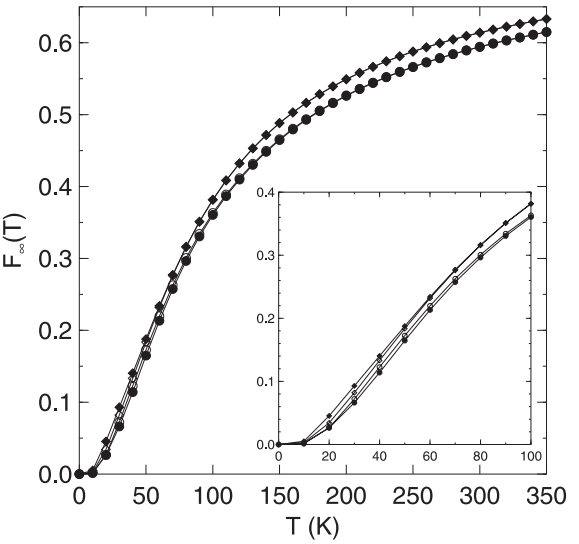

Fig. 3. Temperature dependence of the F_{∞} function in the case of the spin ladder with (•) and without periodic (○) conditions, and in the case of the dimer chain model with (♦) and without (◊) periodic conditions. The inset allows to emphasize the slightly different behaviours encountered at low temperatures.

With these approximations, Eq. (8) now reads

$$\delta^K_{\text{para}}(T) = \Sigma_K \frac{\mathscr{C} F_{\infty}(T)}{T} = \Sigma_K \hat{\delta}_{\text{para}}(T), \tag{9}$$

with $K =$ I–IV and

$$\begin{aligned} \Sigma_{\text{I}} &= 2A_1^+ + A_3^+ + A_4^-, \\ \Sigma_{\text{II}} &= 2A_1^- + A_3^- + A_4^+, \\ \Sigma_{\text{III}} &= 2A_2^+ + A_3^- + A_4^+, \\ \Sigma_{\text{IV}} &= 2A_2^- + A_3^+ + A_4^-. \end{aligned} \tag{10}$$

The sums Σ_K are given by the fit of ^{31}P NMR data through the use of the formulae

$$\delta^K_{\text{exp}}(T) = \delta^K_{\text{dia}} + \Sigma_K \hat{\delta}_{\text{para}}(T), \ (K = \text{I–IV}) \tag{11}$$

δ^K_{exp} represents the experimental data for the phosphorus atoms of type K, and δ^K_{dia} their diamagnetic shift. In order to proceed, we used the experimental data set published by Tuel. Measurements were done at six different temperatures in the 150–300 K temperature range and 24 points were thus obtained. We performed the adjustment by minimizing the function

$$\mathscr{R} = \frac{1}{N-n}\frac{\sum_{K=\mathrm{I}}^{\mathrm{IV}}\sum_i\left[\delta^K_{\mathrm{exp}}(T_i)-(\delta^K_{\mathrm{dia}}+\hat{\delta}_{\mathrm{para}}(T_i)\,\Sigma_K)\right]^2}{\sum_{K=\mathrm{I}}^{\mathrm{IV}}\sum_i\left[\delta^K_{\mathrm{exp}}(T_i)\right]^2}, \tag{12}$$

where $N = 24$ is the number of experimental points, and $n = 8$ is the number of parameters used. However, the ^{31}P NMR spectra recorded by Yamauchi et al. in the temperature range 4–300 K indicate at low temperatures that the different types of ^{31}P nuclei have very close diamagnetic shifts (about −150 ppm). This allowed us to significantly decrease n to 5 by constraining the diamagnetic shift parameters to take a common value δ_{dia}.

Fig. 4 shows the temperature dependence of the ^{31}P NMR shifts and the curves resulting from the fits.

As can be noted, a reasonably good agreement with the experimental data has been achieved. Remarkably, this is the case with the spin ladder model as well as with the dimer chain model. The values obtained for the parameters and the residues $\mathscr{R}$ are given in Table 2.

For each model, we can see that the presence or absence of periodic conditions leads to similar results. We note also that fits are slightly better with the dimer chain model than with the spin ladder one, whereas the sums Σ are of the same order of magnitude. However, there is a small drop in the values of these constants of approximatively 2 MHz when going from the spin ladder model to

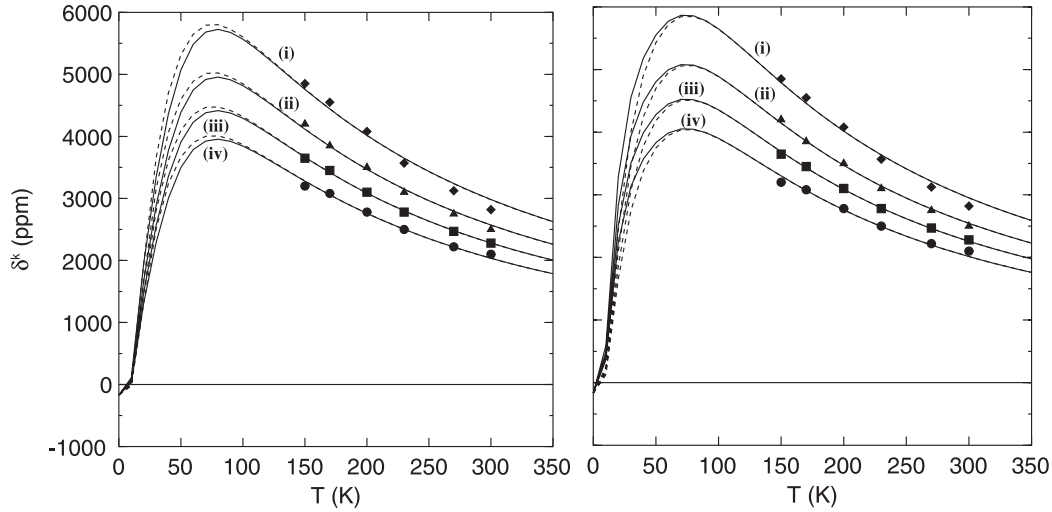

Fig. 4. Adjustment of the VPO ^{31}P NMR data in the case of the spin ladder model (left) and in the case of the dimer chain model (right), with (solid lines) and without (dashed lines) periodic conditions.

Table 2
Results obtained by the adjustment of the ^{31}P NMR data in the frameworks of the spin ladder model and the dimer chain model

	Spin ladder		Dimer chain	
	No periodicity	Periodicity	No periodicity	Periodicity
$\mathscr{R}$	0.0045	0.0045	0.0039	0.0039
$\Sigma_{\mathrm{I,II}}$ (MHz)	61.1, 53.1	61.2, 53.2	58.6, 51.0	58.7, 51.0
$\Sigma_{\mathrm{III,IV}}$ (MHz)	47.5, 42.8	47.6, 42.8	45.6, 41.0	45.6, 41.0
δ_{dia} (ppm)	−167.0	−168.8	−168.2	−168.8

the dimer chain model. This is due to the fact that the F_∞ function takes higher values when evaluated in the framework of the dimer chain model than when calculated in the framework of the spin ladder model (Fig. 3).

It is obvious that we cannot obtain from our fits the values of the hyperfine coupling constants since we have only four linear combinations (Σ_K, $K = \mathrm{I–IV}$) for eight unknown parameters (A_i^ϵ, $i = 1–4$, $\epsilon = \pm$).

Recent works on the dimer chain model indicate that the privileged exchange pathways correspond to the exchange interactions through O–P–O bridges [8,20]. If these pathways correspond to the most important transfer of the spin density, the hyperfine constants $A_1^\pm$ and $A_2^\pm$ are predominating in the sums Σ_K. Since hyperfine interaction generally decreases with the distance between the nucleus and paramagnetic centers involved in the interaction, we can assume that the inequality $A_1^\pm > A_2^\pm$ is verified. In this case, we have the relations

$$\begin{aligned} &\Sigma_{\mathrm{I}} \approx 2A_1^+, \quad \Sigma_{\mathrm{II}} \approx 2A_1^-, \\ &\Sigma_{\mathrm{III}} \approx 2A_2^+, \quad \Sigma_{\mathrm{IV}} \approx 2A_2^-, \end{aligned} \tag{13}$$

where the assignments for Σ_{I}, Σ_{II} on the one hand, and Σ_{III}, Σ_{IV} on the other hand, are arbitrary since we cannot distinguish the constant A_i^+ from the constant A_i^-. So, using the fitted values of the parameters Σ_{k} for the dimer chain model (Table 2), we obtain the highest values allowable for the hyperfine constants $A_1^\pm$ and $A_2^\pm$ within this model framework:

$$\begin{aligned} &A_1^\pm \approx 29;26\mathrm{MHz} \\ &A_2^\pm \approx 23;21\mathrm{MHz} \qquad (A_3^\pm = A_4^\pm \approx 0) \end{aligned} \tag{14}$$

To our knowledge, this is the first time, estimates of hyperfine coupling constants are given for the $(VO_2)P_2O_7$ system.

Our fit is limited by the 150–300 K temperature range used to probe the spin ladder and dimer chain models. The recent ^{31}P NMR studies of Yamauchi et al. covered the more important temperature range 4–300 K [14]. Their low temperatures data reveal that all four signals have a broad maximum around 80 K which is also displayed by the curve of the bulk susceptibility plotted against the temperature [2]. The theoretical signals we have computed present also such a maximum (Fig. 4): in the case of the spin ladder model with or without periodic conditions, the maximum is located at 80 K; in the case of the dimer chain model, it is located at 70 K when periodic conditions are used and 80 K when they are not used.

Yamauchi et al. have shown that the four types of ^{31}P signal can be divided into two families: the first corresponds to the two types of nucleus resonating at higher fields, the second consists of the two types resonating at lower fields. Within each family, both types of signal show the same behaviour at low temperatures. Such phenomenon has been interpreted by the presence of two types of dimer chain in VPO; this model was called the double gap model (as it explains the two singlet–triplet gaps observed by inelastic neutron scattering experiments [9]). One chain, referred to as chain A, is the one we have used for our studies; it is associated with the exchange coupling constants $(J_1^A, J_2^A) = (119, 101\ \mathrm{K})$. The second chain, referred to as chain B, is associated with the exchange coupling constants $(J_1^B, J_2^B) = (130, 90\ \mathrm{K})$. In order to probe the double gap model, additional parameters are needed to distinguish the hyperfine coupling interactions arising from one chain or the other. Within this model framework, one can readily show that the expression Eq. (9) for the paramagnetic shift takes the form

$$\delta^K_{\mathrm{para}}(T) = \frac{\mathscr{C}}{T}\left[\sigma_K^A F_\infty^A(T) + \sigma_K^B F_\infty^B(T)\right], \tag{15}$$

where superscripts A and B refer to the contributions arising from chains A and B and where parameters σ_K^X $(X = A, B)$ admit one of the following four expressions: $\sigma_K^X \in \{2A_{1,2}^\pm(X), 2A_3^\pm(X) + 2A_4^\mp(X)\}$. For both chains, we have evaluated the $F_\infty(T)$ functions with the exchange parameters proposed in [14]. They are plotted on Fig. 5.

One notes on Fig. 5 that the functions differ at low temperatures and that, as expected, the function corresponding to the chain A (with the smaller gap) takes higher values than the function corresponding to chain B (with the larger gap).

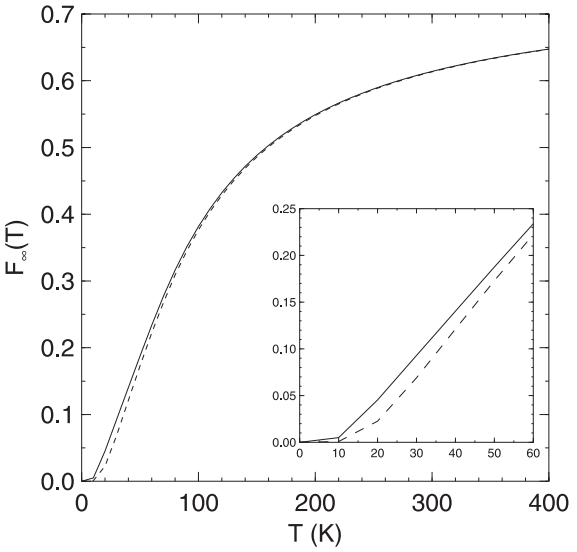

Fig. 5. Temperature dependence of the F_∞ function for chain A (solid line) and chain B (dashed line) in the case of the double gap model (periodic conditions were used).

Spin density increases with temperature faster on chain A than on chain B. One notes also that the contributions from both chains are identical at high temperatures. Such observation implies that we cannot have further informations using the double gap model to analyze the data measured in the 150–300 K temperature range Nevertheless, since we have at high temperatures $F_\infty^A(T) \cong F_\infty^B(T)$, we can establish the following equalities: $\Sigma_k \cong \sigma_k^A + \sigma_k^B, (k = \text{i–iv})$, where the parameters Σ_k are those obtained within the framework of the dimer chain model (Table 2).

It is clear that models such as spin ladder and dimer chain, or even double gap model, remain comparatively simple regarding the structural features of VPO. In fact, exchange parameters do not depend only on V–V distances as it was proposed in [14]. It was shown for different V(+IV) systems with oxo, arsenate and phosphate bridges that they strongly depend on small angle variations [21,22]. Therefore, if one takes into account the structural details, it becomes necessary to introduce more than two exchange parameters, even for a single chain, in order to give an accurate description of the VPO system.

4. Conclusion

Taking into account the exchange interactions in the paramagnetic system $(VO_2)P_2O_7$, we were able to analyze its ^{31}P NMR data over the 150–300 K temperature range. Using the P–V distances and the orientation of the vanadyl groups as criteria, we have identified four different types of phosphorus atom and defined for them dominating hyperfine interactions. We have fitted the experimental data within the spin ladder model framework as well as within the dimer chain model framework. The satisfactory agreement between theory and experiments obtained for both models did not allow us to favour any of the concurrent models. However, we were able to give estimates for the hyperfine coupling constants.

Further work on the analysis of ^{31}P NMR and other magneto–chemical data for the VPO system should consider fine structural–magnetic correlations. In our forthcoming publications, we will give a quantum–chemical analysis of the exchange interactions in VPO which will allow us to refine the spin model of this system.

Acknowledgements

We are grateful to A. Tuel for providing us with the NMR data and for useful discussions. We thank S. Caldarelli for numerous discussions and T. Yamauchi for the reprints of publications.

Appendix A. Exact numerical evaluation of the functions F_i

In order to evaluate the functions F_i (Eq. 3), we need to know the eigenvalues E_n and the eigenfunctions $|S_n\rangle$ of the system Hamiltonian. We also need to evaluate the projection coefficients $K_i(n)$ Eq. (2). The main difficulty encountered when evaluating these coefficients is related to the calculation of the matrix elements $\langle S_n|\vec{s}_i \cdot \vec{S}|S_n\rangle$. They get calculated in two steps. Firstly, we use the fact that the matrix of the operator $\vec{s}_i \cdot \vec{S}$ is diagonal when expressed in the orthonormal basis

$\{|(s_i, S_{\bar{i}})S\rangle\}$ ($\vec{S}_{\bar{i}} = \sum_{k\neq i} \vec{s}_k = \vec{S} - \vec{s}_i$); the non vanishing matrix elements read $[S(S+1) - s_i(s_i+1) - S_{\bar{i}}(S_{\bar{i}}+1)]/2$. Secondly, $\langle S_n|\vec{s}_i \cdot \vec{S}|S_n\rangle$ is obtained by a simple change of basis.

We do not have to calculate all functions F_i because of the presence of symmetry properties in the studied systems. Let us consider the subspace $\mathscr{E}_n$, possibly d–fold degenerated, corresponding to the level of energy E_n. Let us note $\{|S_n^{(k)}\rangle\}$ ($k = 1, \ldots, d$) an orthonormal basis of $\mathscr{E}_n$ made of the system's Hamiltonian eigenfunctions. The contribution C_i^n of this subspace to F_i is given by

$$C_i^n(T) = \left(\sum_{k=1}^{d} \langle S_n^{(k)}|\vec{s}_i \cdot \vec{S}|S_n^{(k)}\rangle\right) \times \frac{(2S_n+1)\exp(-E_n/k_BT)}{\sum_p (2S_p+1)\exp(-E_p/k_BT)}.$$

The sum ($\sum_{k=1}^{d} \langle S_n^{(k)}|\vec{s}_i \cdot \vec{S}|S_n^{(k)}\rangle$) is the trace of the operator $\vec{s}_i \cdot \vec{S}$ restricted to $\mathscr{E}_n$. We consider a site j related to site i through a symmetry operation whose operator is noted $\mathscr{P}$. We verify for the fundamental observables $\vec{s}_i$ and its transformed by $\mathscr{P}$ $\vec{s}_i{}'$ the relation [23]: $\vec{s}_i{}' = \mathscr{P}\vec{s}_i\mathscr{P}^\dagger$, which gives $\vec{s}_j = \mathscr{P}\vec{s}_i\mathscr{P}^\dagger$, sites i and j being equivalent. Since the total electronic spin $\vec{S}$ is unchanged by carrying out the symmetry operation, the same relation holds for $\vec{S}$:$\vec{S} = \mathscr{P}\vec{S}\mathscr{P}^\dagger$. We thus obtain the equality

$$\sum_{k=1}^{d} \langle S_n^{(k)}|\vec{s}_j \cdot \vec{S}|S_n^{(k)}\rangle = \sum_{k=1}^{d} [\langle S_n^{(k)}|\mathscr{P}](\vec{s}_i \cdot \vec{S})[\mathscr{P}^\dagger|S_n^{(k)}\rangle].$$

The right member of this equality is the trace of the operator $\vec{s}_i \cdot \vec{S}$ restricted to the subspace generated by the orthonormal set of functions $\mathscr{P}^\dagger|S_n^{(k)}\rangle$. Because $\mathscr{P}^\dagger$ and the system Hamiltonian commute, the subspace $\mathscr{E}_n$ is globally invariant under the action of $\mathscr{P}^\dagger$ and admits $\{\mathscr{P}^\dagger|S_n^{(k)}\rangle\}$ as an orthonormal basis. Therefore, the trace of an operator being independent of the basis choice, the right member of the equality above is the trace of $\vec{s}_i \cdot \vec{S}$ restricted to $\mathscr{E}_n$. We thus have

$$\sum_{k=1}^{d} \langle S_n^{(k)}|\vec{s}_j \cdot \vec{S}|S_n^{(k)}\rangle = \sum_{k=1}^{d} \langle S_n^{(k)}|\vec{s}_i \cdot \vec{S}|S_n^{(k)}\rangle.$$

Consequently, if sites i and j are equivalent, we verify: $F_i = F_j$.

If we consider infinite systems (spin ladder or dimer chain), all sites are related to each other through symmetry operations (translations and reflections): the F_i functions are all equivalent to a unique one. The same holds for finite clusters with periodic conditions. In the case of finite clusters modeling dimer chain, there exists a bisecting symmetry plane. In the case of finite clusters modeling spin ladder, there exists two orthogonal bisecting symmetry plane.

References

[1] G. Centi, Forum on vanadyl pyrophosphate catalysts, (special issue) Catal. Today 16, 1993, 1–147, and references therein.
[2] D.C. Johnston, J.W. Johnson, D.P. Goshorn, A.J. Jacobson, Phys. Rev. B 35 (1987) 219.
[3] E. Dagotto, J. Riera, D. Scalapino, Phys. Rev. B 45 (1992) 5744.
[4] T. Barnes, E. Dagotto, J. Riera, E.S. Swanson, Phys. Rev. B 47 (1993) 3196.
[5] R.S. Eccleston, T. Barnes, J. Brody, J.W. Johnson, Phys. Rev. Lett. 73 (1994) 2626.
[6] M. Troyer, H. Tsunetsugu, D. Würtz, Phys. Rev. B 50 (1994) 13515.
[7] T. Barnes, J. Riera, Phys. Rev. B 50 (1994) 6817.
[8] M. Roca, P. Amorós, J. Cano, M.D. Marcos, J. Alamo, A. Beltrán-Porter, D. Beltrán-Porter, Inorg. Chem 67 (1998) 3167.
[9] A.W. Garrett, S.E. Nagler, D.A. Tennant, B.C. Sales, T. Barnes, Phys. Rev. Lett. 79 (1997) 745.
[10] G.S. Uhrig, B. Normand, Phys. Rev. B 58 (1998) R14705.
[11] M.R. Thompson, A.C. Hess, J.B. Nicholas, J.C. White, J. Anchell, J.R. Ebner, in: V.C. Corberán, S.V. Bellón, (Eds.), New Developments in Selective Oxidation II, Elsevier, Amsterdam, 1994, 167.
[12] J. Li, M.E. Lashier, G.L. Schraeder, B.C. Gerstein, Appl. Catal. 73 (1991) 1323.
[13] M.T. Sananes, A. Tuel, Solid State NMR 6 (1996) 157.
[14] T. Yamauchi, Y. Narumi, J. Kikuchi, Y. Ueda, K. Tatani, T.C. Kobayashi, K. Kindo, K. Motoya, Phys. Rev. Lett. 83 (1999) 3729.
[15] I. Bertini, C. Luchinat, NMR of Paramagnetic Molecules in Biological Systems, Benjamin/Cummings, Menlo Park, CA, 1986.
[16] I. Bertini, C. Luchinat, Coord. Chem. Rev. 150 (1996) 1.
[17] V. Robert, S. Petit, S.A. Borshch, B. Bigot, J. Phys. Chem. A 104 (2000) 4586.
[18] Y.E. Gorbunova, S.A. Linde, Sov. Phys. Dokl. 24 (1979) 138.

[19] P.T. Nguyen, R.D. Hoffman, A.W. Sleight, Mater. Res. Bull. 30 (1995) 1055.
[20] D. Beltrán-Porter, P. Amorós, R. Ibáñez, E. Martínez, A. Beltrán-Porter, A. LeBail, G. Ferey, G. Villeneuve, Solid State Ionics 32 (1989) 57.
[21] D. Gatteschi, L. Pardi, A.-L. Barra, A. Müller, in: M.T. Pope, A. Müller, (Eds.), Polyoxometalates: From Platonic Solids to Anti–Retroviral Activity, Kluwer, Dordrecht, 1994, 219.
[22] A. Müller, F. Peters, M.T. Pope, D. Gatteschi, Chem. Rev. 98 (1998) 239.
[23] A. Messiah, Mécanique quantique, vol. 2, Dunod, Paris, 1995, XV-6, p. 550.